Low-light-level cross-phase modulation by quantum interference

Hsiang-Yu Lo, Po-Ching Su, and Yong-Fan Chen*
Department of Physics, National Cheng Kung University, Tainan 701, Taiwan, Republic of China
(Received 18 March 2010; published 18 May 2010)

We report on the direct measurement of low-light-level cross-phase modulation (XPM) based on electromagnetically induced transparency (EIT) in the pulsed regime. A phase shift of 0.02 rad of a probe pulse modulated by a signal pulse with a peak intensity of 3 μW/cm^2 was observed, which is the lowest intensity ever achieved for the N-type EIT-based XPM system. The experimental data make a quantitative prediction of the single-photon-level XPM phase shift arising from two interacting pulses with unequal group velocities that is consistent with the theoretical predictions proposed by Harris and Hau [Phys. Rev. Lett. **82**, 4611 (1999)]. Furthermore, a proof-of-principle experiment demonstrating an enhancement of the nonlinear optical Kerr effect by shining the signal pulse twice is presented.

DOI: 10.1103/PhysRevA.81.053829 PACS number(s): 42.50.Gy, 42.25.Hz, 32.80.Qk, 03.67.−a

I. INTRODUCTION

The nonlinear optical process, which enables photon-photon interaction, plays an important role in quantum information processing. Kerr nonlinearity at the few-photon level is promising for applications to quantum nondemolition measurement [1], quantum logic gates [2], and generation of quantum entangled states [3]. The strength of the interaction between two photons is extremely weak; hence, intense optical fields are usually required to achieve a practical nonlinear effect. A nonlinear phase shift of one field modulated by another is referred to as cross-phase modulation (XPM). A four-level XPM scheme based on electromagnetically induced transparency (EIT) [4,5] has attracted considerable attention since it was reported by Schmidt and Imamoğlu in 1996 [6]. In 2003, Kang and Zhu observed a nonlinear phase shift of 0.13 rad induced by a signal field with an intensity of 1.8 mW/cm^2 in an EIT-based XPM scheme [7].

However, the four-level XPM system has an ultimate limit at the single-photon level that was theoretically analyzed for the case of one slow pulse that arises from EIT and another fast pulse that propagates at the speed of light [8]. Several studies have proposed approaches for achieving more efficient XPM [3,9–14]. Nevertheless, most experiments on the pulsed regime are only in their infancy because of complexity and stringent conditions. Recently, Gorshkov *et al.* [15] proposed that a single-photon π phase shift can be achieved via an exchange of fermionic spin excitations [16]. To date, nonlinear phase shifts at the single-photon level have been performed in cavity quantum electrodynamics-based devices [2,17] and in optical fiber [18]. The EIT-based XPM is still one of the best candidates for realizing few-photon applications in quantum science and technology. Accordingly, research on low-light-level XPM based on EIT in the pulsed regime is important as it can be used to carry out the protocol for quantum logic gates between photonic qubits [19,20].

II. EXPERIMENTAL DETAILS

In the present study, EIT-based XPM is investigated using an N-type atomic system. The relevant energy levels of ^{87}Rb atoms are shown in Fig. 1(a). In our experiment, a typical cloud of 3×10^9 cold atoms was prepared in a magneto-optical trap (MOT), as measured by the optical-pumping method. The principal element in the N-type XPM system is a three-level Λ-scheme EIT subsystem. For this subsystem, a weak probe and strong coupling fields are employed to drive the D_2 transitions of $|F=1\rangle \equiv |1\rangle \leftrightarrow |F'=2\rangle \equiv |3\rangle$ and $|F=2\rangle \equiv |2\rangle \leftrightarrow |3\rangle$, respectively. Here, the probe and coupling fields are circularly polarized with $\sigma+$ polarization; they propagate in nearly the same direction ($\theta < 1^\circ$). The XPM or equivalent to Kerr nonlinearity is performed by applying a signal field that drives the $|2\rangle \leftrightarrow |F'=3\rangle \equiv |4\rangle$ transition [see Fig. 1(a)]. The signal field, which is $\sigma-$ polarized, copropagates with the coupling field. The probe, coupling, and signal fields form a typical N-type XPM based on the EIT scheme.

The scheme of the experimental setup is shown in Fig. 1(b). The probe and coupling fields come from two diode lasers, respectively. The coupling laser is directly injection locked by an external cavity diode laser (ECDL). One beam from the ECDL is sent through a 6.8-GHz electro-optic modulator (EOM, New Focus 4851). The probe laser is injection locked by an intermediate laser seeded with the high-frequency sideband of the EOM output. The above arrangement can completely eliminate the influence of the carrier of the EOM output on the probe laser. The signal field is directly generated from this ECDL. The probe and coupling fields are first combined with a 50:50 beam splitter (BS1). Next, the coupling field is overlapped with the signal field on a polarization beam splitter (PBS1). The three fields are circularly polarized with a quarter-wave plate (QWP) and then injected into the atomic sample. After leaving the atomic cloud, the coupling and signal fields pass a second QWP, which converts the circular polarizations into original linear polarizations; they are then directed onto the photodetector (PD3). Furthermore, a beat-note interferometer is used to directly and simultaneously measure the phase shift and transmission of the probe pulse [21].

In the system of the beat-note interferometer, the probe laser is first split into the transmitted and reflected beams by BS2. The transmitted beam passes the acousto-optic modulator (AOM) to generate a first-order beam (1°) for the probe pulse and then recombines with the reflected beam (0°) on BS3. After

*yfchen@mail.ncku.edu.tw

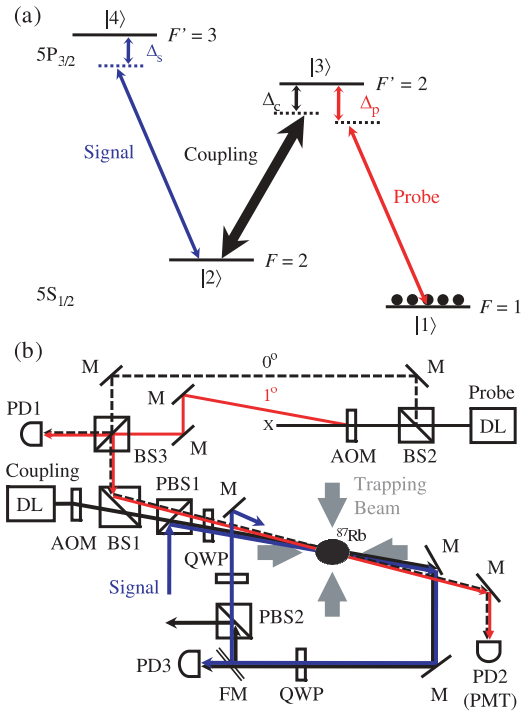

FIG. 1. (Color online) (a) Four-level XPM system and relevant energy levels in ^{87}Rb D_2 line. The coupling and probe fields form the Λ-configuration EIT subsystem. (b) A schematic diagram of the experimental setup. BS, beamsplitter; PBS, polarization beamsplitter; QWP, quarter-wave plate; AOM, acousto-optic modulator; PD, photodetector; PMT, photomultiplier tube; M, mirror; FM, flip mirror.

leaving BS3, one beam is called the reference beat notes, which is directly received by PD1, and the other one, corresponding to the probe beat notes, is detected by PD2 after interacting with atoms. Here, the input powers of the zeroth- and first-order beams for the probe beat notes are fixed at 2 nW and 500 pW, respectively. The driving frequency, ω_a, of the AOM in our experiment is $2\pi \times 80$ MHz, which is sufficiently large that the interaction between the zeroth-order beam and the sample is negligible. Both the reference and probe beat notes carry a beat frequency of ω_a. The phase shift of the probe pulse is measured by directly comparing the two beat signals using an oscilloscope. At the same time, the probe transmission can be obtained from the amplitude of the probe beat notes. Only the phase shift within 200 ns of the end of the probe pulse is considered in order to neglect the transient effect in XPM and to acquire steady-state results. Details of the above method can be found in Ref. [22].

The timing sequence in the experiment is described below. The magnetic field of the MOT is first switched off. After a 1.4-ms delay, the repumping laser of the MOT is switched off, the coupling field is switched on, and then the trapping beams of the MOT are turned off to ensure that the entire population is optically pumped to the ground state $|1\rangle$. When all the fields of the MOT are turned off, the 15-μs probe square pulse and the 20-μs signal square pulse are turned on simultaneously. The above sequence is repeated at a period of 10 ms. Throughout the experiment, the statistical error bar is evaluated using 10 samples, with each sample averaged 2048 times using an oscilloscope.

III. THEORETICAL MODEL

An effective non-Hermitian Hamiltonian, which incorporates three decay channels into the original Hermitian component, is used to calculate the Kerr nonlinearity in the N-type XPM system

$$\begin{aligned}\hat{H}_{\text{eff}} = &-\frac{\hbar}{2}(\Omega_p\hat{\sigma}_{31} + \Omega_c\hat{\sigma}_{32} + \Omega_s\hat{\sigma}_{42} + \text{H.c.}) \\ &+\hbar\left(-\Delta_p - i\frac{\gamma_{31}}{2}\right)\hat{\sigma}_{33} + \hbar\left(-\delta - i\frac{\gamma_{21}}{2}\right)\hat{\sigma}_{22} \\ &+\hbar\left(-\Delta - i\frac{\gamma_{42}}{2}\right)\hat{\sigma}_{44}, \end{aligned} \tag{1}$$

where $\hat{\sigma}_{ij}$ is the atomic projection operator ($i,j = 1,2,3,4$). Ω_p, Ω_c, and Ω_s are the Rabi frequencies of probe, coupling, and signal transitions, respectively. $\Delta_p \equiv \omega_p - \omega_{31}$ is the one-photon detuning, $\delta \equiv (\omega_p - \omega_c) - \omega_{21} \equiv \Delta_p - \Delta_c$ is the two-photon detuning, and $\Delta \equiv (\omega_p - \omega_c + \omega_s) - \omega_{41} \equiv \delta + \Delta_s$ is the three-photon detuning. Here, $\gamma_{21} \equiv \gamma_{2\text{deph}}$, $\gamma_{31} \equiv \Gamma_3 + \gamma_{3\text{deph}}$, and $\gamma_{42} \equiv \Gamma_4 + \gamma_{4\text{deph}}$ represent the total coherence decay rates. Γ_3 and Γ_4 are the spontaneous decay rates out of excited states $|3\rangle$ and $|4\rangle$. The energy-conserving dephasing processes with rates $\gamma_{2\text{deph}}$, $\gamma_{3\text{deph}}$, and $\gamma_{4\text{deph}}$ are also included in the above model. The Schrödinger equation is then solved with the effective Hamiltonian of Eq. (1) to yield equations of motion for the population amplitudes. The probe field is treated as a perturbation to obtain the steady-state solution of the susceptibility, χ, of the probe field. The imaginary part of χ characterizes the absorptive properties of the medium; hence, the intensity transmission of probe field is $T = \exp[-\text{Im}(\chi)kL]$, where k is the wave number of the probe field, L is the optical path length of the medium, and $\text{Im}(\chi)kL$ is the power loss of the probe field. The real part determines the refractive index of the medium for the probe field, and the XPM phase shift is described as $\Delta\varphi_{\text{XPM}} = \frac{1}{2}\text{Re}(\chi)kL$. Under the condition of $\Delta_p = \delta = 0$, the transmission and phase shift of the probe field in the N-type XPM system are

$$T = \exp\left[-n\sigma_{13}L\gamma_{31}\frac{|\Omega_s|^2(|\Omega_c|^2\gamma_{42} + |\Omega_s|^2\gamma_{31} + 2\gamma_{21}\gamma_{31}\gamma_{42}) + \gamma_{21}(|\Omega_c|^2 + \gamma_{21}\gamma_{31})(4\Delta_s^2 + \gamma_{42}^2)}{4\Delta_s^2(\gamma_{21}\gamma_{31} + |\Omega_c|^2)^2 + (\gamma_{21}\gamma_{31}\gamma_{42} + |\Omega_c|^2\gamma_{42} + |\Omega_s|^2\gamma_{31})^2}\right], \tag{2}$$

$$\Delta\varphi_{\text{XPM}} = -n\sigma_{13}L\gamma_{31}\frac{|\Omega_c|^2|\Omega_s|^2\Delta_s}{4\Delta_s^2(\gamma_{21}\gamma_{31} + |\Omega_c|^2)^2 + (\gamma_{21}\gamma_{31}\gamma_{42} + |\Omega_c|^2\gamma_{42} + |\Omega_s|^2\gamma_{31})^2}, \tag{3}$$

where n is the density of the medium, σ_{13} is the atomic cross section of the $|1\rangle \leftrightarrow |3\rangle$ transition, and $n\sigma_{13}L$ is the optical density for the probe transition. From the calculation results, the EIT-based XPM can be understood that the signal field induces an ac-Stark shift of the ground state $|2\rangle$ to perturb the EIT medium away from two-photon Raman resonance. This breaks the EIT resonance requirement and introduces nonlinear absorption and refraction into the medium. The figure of merit, ζ, for the XPM scheme is defined as the ratio of the probe phase shift to its power loss; it is given by

$$\zeta = \frac{-|\Omega_c|^2|\Omega_s|^2\Delta_s}{|\Omega_s|^2(|\Omega_c|^2\gamma_{42} + |\Omega_s|^2\gamma_{31} + 2\gamma_{21}\gamma_{31}\gamma_{42}) + \gamma_{21}(|\Omega_c|^2 + \gamma_{21}\gamma_{31})\left(4\Delta_s^2 + \gamma_{42}^2\right)}. \tag{4}$$

ζ is independent of the optical density and depends on γ_{21}, Ω_s, and Ω_c. Of note, ζ does not linearly increase with Δ_s, and it has a maximum value when $\gamma_{21} \neq 0$. The significance of ζ is that it determines the ultimate efficiency of EIT-based XPM at the single-photon level. This parameter is further discussed below.

IV. RESULTS AND DISCUSSION

Figure 2 shows the probe transmission and nonlinear phase shift as a function of the signal detuning, Δ_s, when both the probe and coupling transitions are on resonance. The experimental data and theoretical predictions are plotted using symbols and solid lines, respectively. The parameters for the theoretical calculations of Eqs. (2) and (3) plotted in Fig. 2 were determined from other experiments. The dephasing rate of the $|1\rangle \leftrightarrow |2\rangle$ transition, γ_{21}, is 0.002Γ, as estimated from the degree of transparency in the EIT spectrum, where $\Gamma = 2\pi \times 6$ MHz is the spontaneous decay rate of the excited states. The Rabi frequency of the coupling transition, Ω_c, is 0.31Γ, as obtained from the separation of two absorption peaks in the EIT spectrum. The optical density is 15.5, as derived from the group delay time of slow light pulses [23]. The total coherence decay rates out of the two excited states, γ_{31} and γ_{42}, are both 1.25Γ, as determined from the spectral width of the one-photon absorption. Furthermore, the Rabi frequency of the signal transition, Ω_s, is determined from the photon switching effect [24]. In Figs. 2(a)–2(d), the Ω_s values are 0.02Γ, 0.05Γ, 0.1Γ, and 0.19Γ, corresponding to 3, 20, 77, and 278 μW/cm^2, respectively. With these reasonable parameters, the experimental data are in good agreement with the theoretical predictions. In particular, the phase shift of 0.02 rad of a probe pulse modulated by a signal pulse with a peak intensity of 3 μW/cm^2, as shown in Fig. 2(a), is the lowest intensity ever achieved in EIT-based XPM. Figure 2 also shows that the characteristics of the EIT enhanced Kerr nonlinearity behave similar to that of the linear susceptibility in the two-level system [25], and Δ_s approaches half of γ_{42} to achieve a maximum phase shift as Ω_s decreases, which is consistent with the theoretical prediction in Ref. [23].

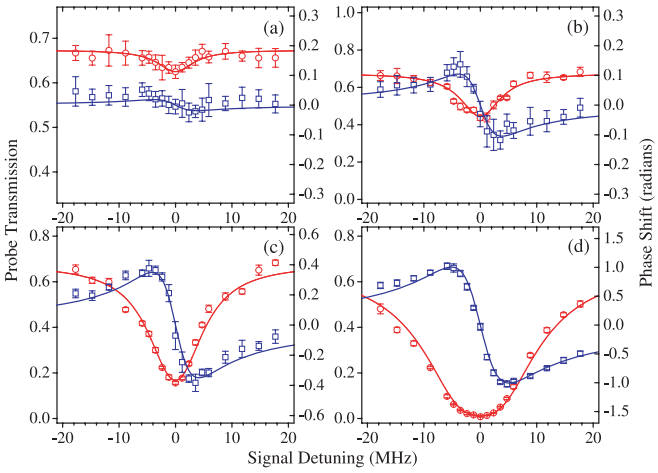

FIG. 2. (Color online) Measured probe transmission (circles) and nonlinear phase shift (squares) versus the signal detuning. Solid lines correspond to the theoretical predictions based on Eqs. (2) and (3). The parameters for the theoretical curves are $n\sigma_{13}L = 15.5$, $\gamma_{21} = 0.002\Gamma$, $\gamma_{31} = \gamma_{42} = 1.25\Gamma$, $\Omega_c = 0.31\Gamma$, and $\Omega_s = 0.02\Gamma$ in (a), 0.05Γ in (b), 0.10Γ in (c), and 0.19Γ in (d).

It is worth noting that our experimental results can make a quantitative prediction of the nonlinear phase shift at the single-photon level. The EIT-based XPM phase shift arising from two interacting pulses with unequal group velocities was discussed and evaluated using the slowly varying envelope equation in Ref. [8], which is given by

$$\Delta\varphi_{\mathrm{XPM}} = -\frac{N_s\sigma_{24}}{A}\left(\frac{\Delta_s\gamma_{42}}{4\Delta_s^2 + \gamma_{42}^2}\right)\psi(\eta), \tag{5}$$

where N_s is the number of photons in the signal pulse, σ_{24} is the atomic cross section of the $|2\rangle \leftrightarrow |4\rangle$ transition, and A is the cross-sectional area of the signal field. $\eta = T_d/T_p$ is the ratio of the probe delay time in the EIT medium to the probe pulse width. The nonlinear phase shift is determined by the parameter $\psi(\eta) = \frac{1}{2}\mathrm{erf}[\frac{\sqrt{4\ln 2}T_p}{T_s}\eta]$, where T_s is the signal pulse width. In our experiment, η and $\psi(\eta)$ are around 0.36 and 0.24, respectively. Thus, the calculated maximum phase shift according to Eq. (5) is 0.06 rad at the conditions of $\Delta_s = \gamma_{42}/2$ and the single-photon signal pulse is focused into an area $A \sim \sigma_{24}$. In Fig. 2(b), the number of photons in the 20-μs signal pulse focused into $A \sim \sigma_{24}$ with a peak intensity of 20 μW/cm^2 was calculated to be 4.5, which made a probe pulse acquire a 0.1-rad phase shift. However, to obtain a maximum probe phase shift of 0.1 rad, the number of photons within the signal pulse should be 1.7 photons according to Eq. (5). This discrepancy is due to the mean Clebsch-Gordan coefficient of the $|2\rangle \leftrightarrow |4\rangle$ transition being around 0.65 in our experiment, not 1 as in the theoretical assumption. The above discussion quantitatively verifies the theoretical analysis for the giant Kerr nonlinearity in which the group-velocity

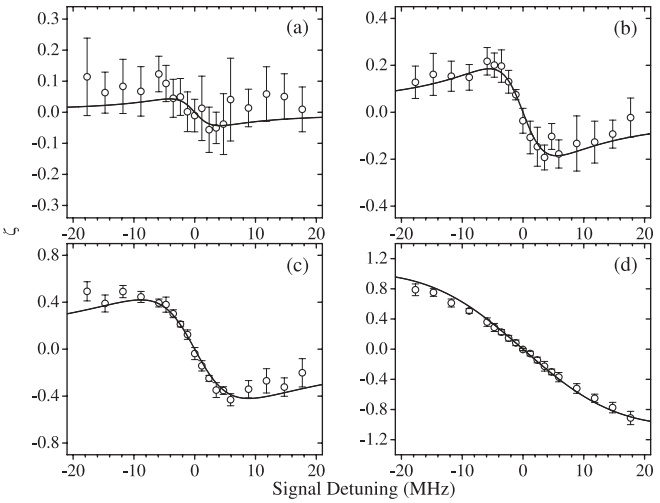

FIG. 3. Cross-phase-modulation figure of merit as a function of signal detuning. Symbols and solid lines represent the experimental data and theoretical curves, respectively. The parameters for the theoretical curves based on Eq. (4) are the same as those in Fig. 2.

mismatch between the probe and signal pulses is taken into account. Equation (5) also shows that the maximum nonlinear phase shift in EIT-based N-type XPM is on the order of 0.1 rad at the single-photon level [23].

The XPM figure of merit, ζ, is plotted as a function of signal detuning, Δ_s, in Fig. 3. Under an ideal condition of zero dephasing rate ($\gamma_{21} = 0$), the ζ value linearly increases with Δ_s [6]. In other words, the figure of merit can always be improved by increasing the signal detuning in the N-type XPM scheme. However, in the case of $\gamma_{21} \neq 0$, ζ has a maximum value because the dephasing rate imposes a limit on EIT transmission of the probe field (see Fig. 3). Therefore, in order to enhance the figure of merit for applications in quantum information processing, the dephasing rate must be made as small as possible, or the Rabi frequency of the coupling transition must be increased. The experimental data also show that the maximum figure of merit appears near $\Delta_s = \gamma_{42}/2$ as the signal intensity decreases. The parameters for the theoretical curves in Fig. 3 based on Eq. (4) are the same as those of Fig. 2. The experimental data are consistent with the theoretical predictions.

The experiment was extended to demonstrate the enhancement of Kerr nonlinearity by shining the signal pulse twice. As shown in Fig. 1(b), a flip mirror (FP) was inserted in front of PD3 to guide the coupling and signal fields. Then, the coupling field is filtered out after passing through PBS2. The signal field is circularly polarized by a QWP and sent back to the EIT medium. Note that the angle between the first and second signal pulses is smaller than 3°. Figure 4 shows the experimental results of probe transmission, nonlinear phase shift, and the corresponding figure of merit as a function of signal detuning. The parameters for the theoretical curves (solid lines) are the same as those in Fig. 2(b) except that Ω_s is replaced by $\sqrt{2} \times 0.05\Gamma$. Compared with Fig. 2(b), the nonlinear phase shift and figure of merit are improved by shining the signal pulse twice. The asymmetry around the far signal detuning in Fig. 4(a) may result from the mismatch of the first and second signal pulses on the atoms.

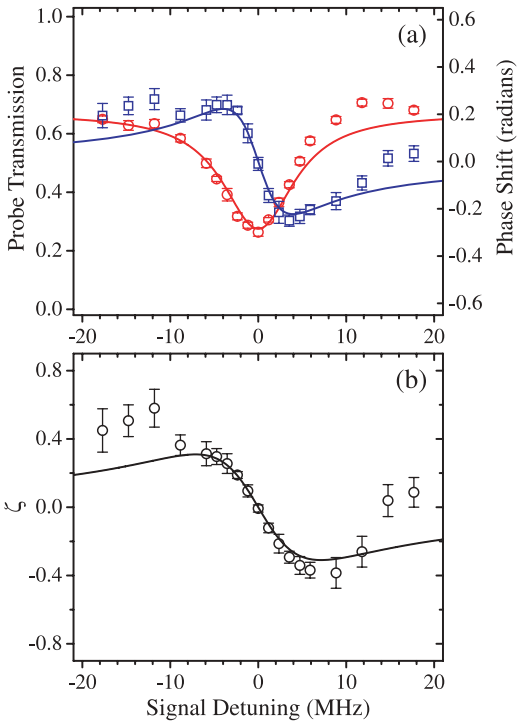

FIG. 4. (Color online) Enhancement of nonlinear Kerr phase shift by shinning the signal pulse twice. (a) Probe transmission (circles) and nonlinear phase shift (squares) versus the signal detuning. (b) The figure of merit versus the signal detuning. The parameters for the theoretical curves (solid lines) are the same as those in Fig. 2(b) except $\Omega_s = \sqrt{2} \times 0.05\Gamma$. The asymmetry around the far signal detuning is possibly ascribed to the mismatch of the first and second signal pulses on the atoms.

V. CONCLUSION

The N-type XPM based on EIT in the pulsed regime was explored. The experimental results are in good agreement with the theoretical predictions. In particular, a phase shift of 0.02 rad of a probe pulse modulated by a signal pulse with a peak intensity of 3 μW/cm^2 was observed, the corresponding number of photons within the signal pulse is about 10^7 in the experiment. The experimental data also indirectly verify theoretical predictions for the single-photon-level XPM phase shift arising from two interacting pulses with unequal group velocities. Furthermore, a proof-of-principle experiment demonstrating an enhancement of the nonlinear optical Kerr effect by shining the signal pulse twice is presented. From the result of shining the signal pulse twice, the EIT-based XPM scheme can be extended to use an optical cavity to increase the nonlinear Kerr effect. This shows that a phase shift of π of one single-photon pulse induced by another may be possible.

ACKNOWLEDGMENTS

We acknowledge Ying-Cheng Chen, Bing He, and Ite A. Yu for helpful discussions. This work was supported by the National Science Council of Taiwan under grants no. 96-2112-M-006-022-MY3, no. 97-2628-M-006-015, and no. 98-2628-M-006-002.

[1] J. P. Poizat and P. Grangier, Phys. Rev. Lett. **70**, 271 (1993).
[2] Q. A. Turchette, C. J. Hood, W. Lange, H. Mabuchi, and H. J. Kimble, Phys. Rev. Lett. **75**, 4710 (1995).
[3] M. D. Lukin and A. Imamoğlu, Phys. Rev. Lett. **84**, 1419 (2000).
[4] S. E. Harris, J. E. Field, and A. Imamoğlu, Phys. Rev. Lett. **64**, 1107 (1990).
[5] K.-J. Boller, A. Imamoğlu, and S. E. Harris, Phys. Rev. Lett. **66**, 2593 (1991).
[6] H. Schmidt and A. Imamoğlu, Opt. Lett. **21**, 1936 (1996).
[7] H. Kang and Y. Zhu, Phys. Rev. Lett. **91**, 093601 (2003).
[8] S. E. Harris and L. V. Hau, Phys. Rev. Lett. **82**, 4611 (1999).
[9] A. Imamoğlu, H. Schmidt, G. Woods, and M. Deutsch, Phys. Rev. Lett. **79**, 1467 (1997).
[10] A. B. Matsko, I. Novikova, G. R. Welch, and M. S. Zubairy, Opt. Lett. **28**, 96 (2003).
[11] Z.-B. Wang, K.-P. Marzlin, and B. C. Sanders, Phys. Rev. Lett. **97**, 063901 (2006).
[12] Y.-F. Chen, C.-Y. Wang, S.-H. Wang, and I. A. Yu, Phys. Rev. Lett. **96**, 043603 (2006).
[13] S. Li, X. Yang, X. Cao, C. Zhang, C. Xie, and H. Wang, Phys. Rev. Lett. **101**, 073602 (2008).
[14] Y. Zhu, Opt. Lett. **35**, 303 (2010).
[15] A. V. Gorshkov, J. Otterbach, E. Demler, M. Fleischhauer, and M. D. Lukin, e-print arXiv:1001.0968v1 [quant-ph].
[16] L.-M. Duan, E. Demler, and M. D. Lukin, Phys. Rev. Lett. **91**, 090402 (2003).
[17] I. Fushman, D. Englund, A. Faraon, N. Stoltz, P. Petroff, and J. Vucković, Science **320**, 769 (2008).
[18] N. Matsuda, R. Shimizu, Y. Mitsumori, H. Kosaka, and K. Edamatsu, Nature Photon. **3**, 95 (2009).
[19] M. A. Nielsen and I. L. Chuang, *Quantum Computation and Quantum Information* (Cambridge University Press, Cambridge, 2000).
[20] B. He, Y.-H. Ren, and J. A. Bergou, J. Phys. B **43**, 025502 (2010).
[21] Y.-F. Chen, Y.-C. Liu, Z.-H. Tsai, S.-H. Wang, and I. A. Yu, Phys. Rev. A **72**, 033812 (2005).
[22] H.-Y. Lo, P.-C. Su, Y.-W. Cheng, P.I Wu, and Y.-F. Chen, submitted for publication (2010).
[23] M. Fleischhauer, A. Imamoğlu, and J. P. Marangos, Rev. Mod. Phys. **77**, 633 (2005).
[24] S. E. Harris and Y. Yamamoto, Phys. Rev. Lett. **81**, 3611 (1998).
[25] S. A. Aljunid, M. K. Tey, B. Chng, T. Liew, G. Maslennikov, V. Scarani, and C. Kurtsiefer, Phys. Rev. Lett. **103**, 153601 (2009).